# Relation between hyperfine field and lattice-location measurements for heavy impurities in iron: Influence of radiation damage*

L. Thomé and H. Bernas
*Institut de Physique Nucléaire, Université Paris-Sud, 91406 Orsay, France*

C. Cohen
*Groupe de Physique des Solides de l'Ecole Normale Supérieure, Université Paris VII, 75221 Paris, France*

(Received 22 May 1978)

The relation between the hyperfine interaction (HFI) and the lattice location of heavy impurities in iron is discussed in the light of results (see companion papers) on $^{169}$Yb, $^{175}$Yb, and Au in Fe. A compilation of all known results in Fe and Cu reveals a simple correlation between the difference in atomic radii of implanted and host atoms and the corrected extinction ratio in lattice-location experiments. A simple model is developed to account simultaneously for the annealing- and implantation-temperature dependence of the impurity HFI and lattice location in Fe between room temperature and 800 K. It is based on existing information concerning the nature and evolution of radiation damage in Fe: Impurity evolution is described in terms of a two-stage process involving (i) vacancy migration towards the impurity and (ii) migration of the impurity-vacancy complex, with the latter stage being much faster than the former. Quantitative agreement is found with our experimental results, as well as with results obtained on other impurities in Fe. It is suggested that the model is applicable in all cases where vacancy motion determines impurity evolution.

## I. INTRODUCTION

This is the fourth in a series[1] of papers dealing with the influence of radiation damage in lattice-location and hyperfine-interaction (HFI) experiments on heavy impurities in iron. We begin with a qualitative discussion of the relation between the HFI and the corrected extinction ratio $\epsilon$ in lattice-location experiments, based on the results of Papers I, II, and III. We then consider the value of $\epsilon$ for heavy impurities implanted at temperatures where radiation damage is stable. A compilation of experimental results leads us to a form of "Hume-Rothery rule" relating $\epsilon$ to the difference between the atomic radii of implanted impurity and host atoms. Relevant information on radiation-damage evolution in Fe, derived from resistivity and electron microscopy sources, is then summarized. On this basis, we present a quantitative analysis of the changes in both $\epsilon$ and the HFI for Yb in Fe as the annealing or implantation temperature varies from room temperature to 850 K. It is suggested that this analysis may also account for the temperature dependence of $\epsilon$ and the HFI of other heavy impurities in metals.

## II. RADIATION-DAMAGE EFFECTS ON THE IMPURITY EXTINCTION RATIO $\epsilon$ AND ON THE HFI

Consider the physical meaning of the corrected extinction ratio on the impurity (denoted $\epsilon$) as defined in III. In the usual formulation, lattice defects due to implantation are ignored; measuring $\epsilon$ along various crystallographic directions and taking flux-peaking effects into account, the fraction of impurities occupying well-defined lattice sites should then be obtained. This is a common interpretation of channeling results on heavy impurities implanted in Fe. It was supported by experiments[2–5] in which the value of $\epsilon$ was found equal to the proportion of implanted-impurity nuclei with a HFI amplitude presumably corresponding to a substitutional lattice site. In several cases (Ca, I, Xe, Yb, Bi in Fe),[3–7] as in the work reported here, the following results were obtained: (i) the measured room-temperature (RT) value of $\epsilon$ is about 0.40–0.60 in all crystallographic directions; (ii) no significant flux-peaking effect is found in angular scans on the impurity; (iii) the half-width $\psi_{1/2}$ of these angular scans is some 10–15% smaller than that of the corresponding scans on the host. The standard interpretation was that about half of the implanted atoms lie in substitutional sites, the other half being either randomly distributed in the unit cell (this is generally recognized as unlikely) or forming some kind of cluster, compound or oxide, whose structure is incoherent with that of the original host lattice. Taken together, the results of I, II, and III lead us to question this simple interpretation. The suggestion[8] that a rare-earth (RE) oxide precipitate could be formed ("internal oxidation"), due to recoil implantation from the surface-oxide layer or to the

 

presence of interstitial oxygen in the bulk of the host crystal, was contradicted by several experiments in which oxygen was implanted below the surface-oxide layer[9] or directly into the RE-implantation layer (see I). In the latter case, the RE-oxygen interaction was shown to affect the HFI and $\epsilon$ in very different ways, and the fraction of displaced RE atoms depended sharply on the ratio of oxygen to RE concentrations, in contrast to the observed dose independence (between $5 \times 10^{12}$ and $10^{15}$ atoms $cm^{-2}$) of $\epsilon$ when no oxygen is implanted. Several Mössbauer experiments on rare-earth implanted iron[10,11] also suggest that the result of Ref. 8 is not reproduced when the implantation energy is significantly higher than the particularly low value (50 keV) used in that case.

It is now a well-established fact that $\epsilon$ and the HFI are both affected by the interaction of the implanted impurity with radiation damage. In the present discussion, the variations of the corrected extinction ratio $\epsilon$ are related to those of the HFI at the RE-impurity nucleus. It is indeed rather surprising that this is at all possible, in view of the different sensitivities of the channeling phenomenon and the HFI to lattice defects around the impurity. If the damage structure is such that the lattice is unperturbed in the near-neighbor shells surrounding the impurity, it is conceivable that the HFI may even have an amplitude corresponding to that of a substitutional atom ($f=1$). This point was discussed in II for the localized RE moment in *Fe* $^{169}$Tm, on which both PAC and Mössbauer-effect results are available. On the other hand, in a channeling experiment the backscattering probability for a particle by an impurity atom depends on the impurity lattice position, but the particle flux *at* the impurity position also depends on the crystal distortions seen by the particle *before* reaching the impurity depth so that the flux, and hence the backscattering probability, may depend rather critically on the size and symmetry of the defect associated with the impurity. This could explain why the room-temperature value of $\epsilon$ for Yb in Fe is reduced well below the expected ($\epsilon=1$) "substitutional" value even if the HFI corresponded to $f=1$ (see II). Of course, if impurity-defect associations are to be considered, the very meaning of a lattice site for an impurity trapped in such a complex must be reexamined.

The analysis of channeling data in a damaged lattice (without impurities) has met with considerable difficulty[12] in all but the simplest[13] cases. If the geometry of the defects is known, analytical or Monte Carlo calculations may be performed in simple cases[14] to assess the modification they induce in the flux distribution of the probing beam. Using this distribution, it may then be possible to deduce quantitative information on the lattice location of impurities lying in an *unperturbed* region of the crystal *beyond* the damaged region. The situation is far more complex when an impurity-defect association has to be considered. A *local* effect is then involved, since the impurity is inside a distorted region of the lattice. The incoming particle flux for each plausible impurity site can only be determined by detailed computer calculation of particle trajectories in the perturbed lattice. The results of such a calculation for various impurity sites could then be compared to the experimental backscattering probability from the impurity. Defect size and shape, as well as the relative position of defect and impurity, will certainly influence the results, and it is likely that rather different configurations will lead to similar backscattering probabilities. For these reasons, such a complex calculation was not attempted in the present work.

## III. RELATION BETWEEN $\epsilon$ AND THE IMPURITY-ATOM RADIUS

Since the room-temperature values of $\epsilon$ are identical in all directions studied, and in the absence of a proper analysis of channeling in the presence of impurity-defect interactions, the correct interpretation of the RT lattice-location results is open to conjecture. However, a systematic study of the literature on lattice location of large impurities in metals leads to an interesting correlation. Lattice-location results have previously been discussed[2] in terms of impurity electronegativity (Darken-Gurry plots). Such a "macroscopic" approach leads to the Hume-Rothery[15] rules for impurity solubility in a metallic host and suggests that the effect of impurity size be investigated. In Figs. 1 and 2 we have plotted the normalized

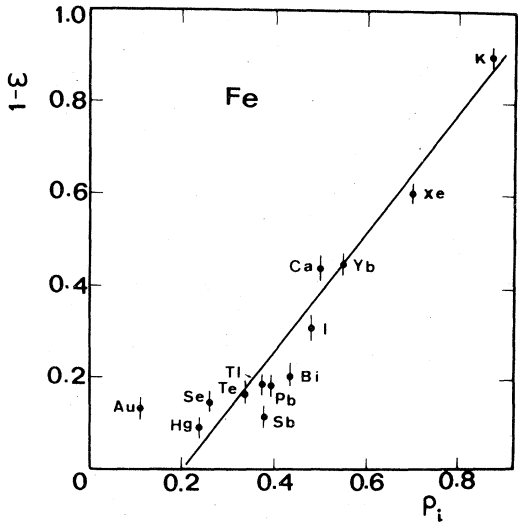


FIG. 1. Values of $1-\epsilon$ as a function of the normalized difference $\rho_i$ between atomic radius of impurities $R_i$ and host $R_0$ for different impurities implanted in iron: $\rho_i=(R_i-R_0)/R_0$. Note that the points are on a straight line for $\rho_i > 0.2$, indicating the critical radius under which an impurity is essentially substitutional.

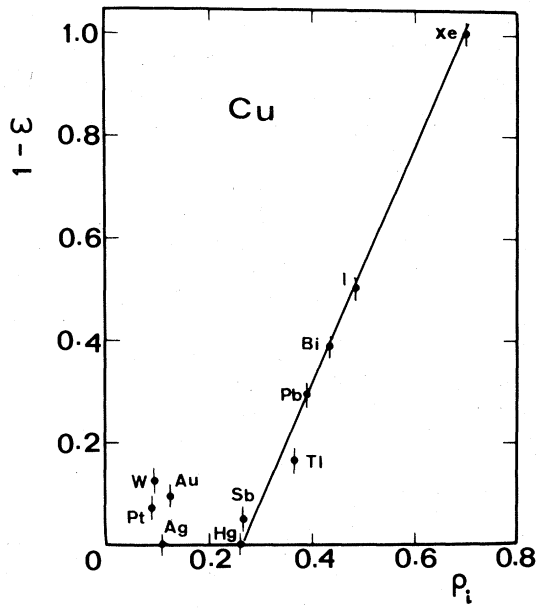


FIG. 2. Values of $1-\epsilon$ as a function of $\rho_i$ (see Fig. 1) for different impurities implanted in copper. Here also, the points are on straight line for $\rho_i > 0.25$.

extinction ratio $\epsilon$ in terms of the difference between impurity ($R_i$) and host ($R_0$) atom radii, for the well-documented cases of Fe and Cu. The results presented in these figures are restricted to impurities of larger atomic radii than host atoms. A linear relation is found between $1-\epsilon$ and $(R_i-R_0)/R_0$: the value of $\epsilon$ is constant and close to unity below a critical radius (when the impurity radius is 20% larger than the host radius for Fe, and 25% larger for Cu). This is a form of "Hume-Rothery rule" for lattice-location experiments: once the critical radius has been determined for a given host, the value of $\epsilon$ is predicted for any large impurity.

Exactly why such a simple relation holds is unclear at present. The difference between host and impurity atomic radii is clearly important to lattice strain, which can affect channeling at the impurity site. It is also essential to the elastic interaction between the impurity and lattice defects such as vacancies or divacancies. However, such effects would presumably induce considerable changes (i.e., narrowing or possibly flux peaking) in the impurity channeling angular distribution. This is not observed (impurity angular distributions are typically only $\lesssim$10–15% narrower than host distributions). To our knowledge, no plausible explanation has yet been offered for this result.

The changes in $\epsilon$ due to annealing or high-temperature implantation reported in this series of papers and elsewhere[3,7,14,16] demonstrate the sensitivity of $\epsilon$ to the impurity-damage interaction, since the effect of the temperature change is to induce point defect detrapping and mobility. As long as no detrapping of the defect from the impurity occurs, and/or as long as the defects interacting with impurities are not mobile, lattice-location results should be temperature independent. For metals of interest here, the latter process sets in at or below 80 K for interstitials and around or above room temperature for vacancies or divacancies. Since several lattice-location experiments[2,17,18] have shown that $\epsilon$ is temperature independent up to at least 300 K, we conclude that *the effect of vacancy (or divacancy) mobility dominates.* Lattice-location results are then determined by the evolution of the impurity-defect interaction as described in Sec. V. As discussed below, the impurity-defect interaction is dose-dependent in that case.

## IV. RELEVANT INFORMATION ON RADIATION DAMAGE IN Fe

Our discussion of the results presented in Papers II and III is based on knowledge of the nature and configuration of radiation damage in Fe. The incoming ion produces[19] a damage cascade, i.e., a distribution of interstitials and vacancies whose detailed structure depends on the deposited energy density. The damage density is such that annihilation of a number of Frenkel pairs[20] takes place. This occurs via an athermal process and may be enhanced thermally by increased vacancy mobility at high temperatures. In view of their low migration energy, interstitials play no further role in damage evolution (beyond this important quasi-instantaneous recombination process) since they migrate very rapidly to the sample surface, to dislocations or to other sinks. On the other hand, resistivity[21] and electron microscopy[22] experiments on quenched Fe showed that vacancies are mobile above room temperature. Stereo-electron-microscopy experiments[23] revealed that room-temperature Yb implantation in Fe at $\gtrsim$100-keV energies produce stable vacancy loops some 100 Å in diameter (no interstitial loops were found) and indicated that these loops are in the (100) planes.[24] After room-temperature implantation, the implanted layer thus contains a network of vacancy loops, a number of isolated vacancies and small vacancy clusters. Resistivity and electron-microscopy results show that sample annealing above 400 K leads to vacancy motion and to vacancy loop growth; when the annealing temperature reaches[21] about 720 K, vacancy clusters begin to anneal out, thus providing an important source of vacancies. Comparatively little knowledge is available on the character of stable defects when the implantation is performed at temperatures above the vacancy mobility threshold (but below the range where void growth phenomena dominate). From existing work[20,23,25] we conclude that mobile vacancies are trapped in large vacancy loops, until the implantation temperature is such that the thermal energy is higher

than the sum of the vacancy migration energy and of the binding energy of the smallest stable cluster, i.e., the mobile vacancy concentration is considerably enhanced when vacancy loops are no longer stable enough to act as the most efficient trap.

Of specific interest to us are the details of the interaction between the various forms of damage and the implanted impurity. To our knowledge, essentially no information is available from established techniques on possible vacancy trapping (or vacancy cluster nucleation) in Fe by implanted impurities, with the exception of the rather detailed studies[26] carried out on rare-gas implants in metals. The latter are particularly relevant to the well-documented combined lattice-location–HFI studies[3,27] on implanted *Fe*Xe but, in view of the very special properties of gases in metals, it is unsafe to generalize the results to RE implants.

The results of Sec. III and the available information[28] on impurity-vacancy interactions in quenched dilute alloys (i.e., where the impurity does *not* create a damage cascade) strongly suggest that although the details of the interaction depend on defect stability, binding, and activation energies, etc., it is in fact determined by the elastic interaction between the vacancy and impurity in a given host. The natural conclusion to draw from the (100) planar effect found in the present *Fe*Yb lattice-location experiments is that *the Yb impurity–defect interaction takes place in the vacancy loop planes,* when it occurs.

## V. INTERPRETATION OF EXPERIMENTAL RESULTS

In this section, we describe a simple calculation that accounts for the evolution of both $\epsilon$ and $f$ in annealing and high-temperature implantation experiments. The main results to account for are (i) the correlated drop in $\epsilon$ and $f$ when room-temperature implanted samples are annealed up to 750 K, in spite of the fact that the implanted does in these experiments differ by a factor $\sim$100; (ii) the noncorrelated change in $\epsilon$ and $f$ in the high-temperature experiments; (iii) the high-temperature values of $\epsilon$ and $f$ in the annealing and hot-implant experiments; and (iv) the privileged effects of the (100) plane in the two series of lattice-location experiments.

### A. General approach

In Paper II, we proposed that the HFI results lead to the conclusion that $f=1$. If this conclusion is correct, it eliminates sites in which the Yb is "precipitated" in one form or another, and for which $\epsilon=0$. However, in view of the remarks of Sec. III, it is not possible to rule out the existence of one or several lattice site(s) for which $f=1$ and $\epsilon \leqslant 1$. For simplicity, we will assume in the following that all Yb-impurities implanted at room temperature land in identical "initial" sites with $f=1$ and $\epsilon=0.56$ (4) in all directions: i.e., the measured value of $\epsilon$ is assigned to *all* impurity sites. If new information proved this value to be an average over different sites, the analysis given here could easily be slightly modified by weighting over the various "initial" sites. It would still hold provided the temperature dependence of the various fractions remains the same.

It is also worth mentioning that the basic features of our analysis do *not* depend on the conclusion (see II) that $f=1$. If the latter were disproved, it would only be necessary to assume that the fraction $1-f$ of implanted nuclei stays constant and does not contribute at all to the observed temperature dependence, i.e., that only the behavior of those ions whose spin is aligned at room temperature is described here. Of course, the numerical results would then be different from those deduced below. The consistency of the present results rather supports, in our view, the contention of II.

Besides this point, our description is based on the following assumptions. (a) Only three possible impurity-lattice sites are considered: initial (site *i*), interacting with a vacancy loop (site *l*) or in a "precipitate" (site *p*). In the present context (as in I–III), the latter is taken in a rather loose sense: it may be in an intermetallic compound or in a very small impurity cluster (e.g., several atoms), such that the requirements described in II for the alignment of the $^{169}$Tm electronic spin are no longer fulfilled. (b) Irreversible transitions from initial sites *i* to sites *l* and *p* may occur after implantation. These transitions are caused by thermal vacancy migration towards impurities. We assume that when a vacancy reaches an impurity, vacancy-assisted migration *immediately* leads to Yb interaction with a vacancy loop (in the temperature range where they exist) or to Yb "precipitation" (above the vacancy-loop stability limit). The evolution of the system is thus dominated by the vacancy diffusion process rather than by the impurity-vacancy complex migration. Finally, (c) in order to simplify calculations the initial distributions of impurities and vacancies in the implantation layer are assumed to be random and uncorrelated, and vacancy migration to sinks is described as a first-order process.

The concentration $c_i$ of impurities remaining in site $i$ at time $t$ may then be written under assumption (b)

$$\frac{dc_i}{dt} = -p_i c_v c_i \tag{1a}$$

(annealing),

$$\frac{dc_i}{dt} = \phi - p_i c_v c_i \tag{1b}$$

(high-temperature implantation), for annealing (1a) and high-temperature implantation (1b) experiments, respectively. In these equations, $\phi$ is the implanta-

tion dose rate, $c_v$ the vacancy concentrations at time $t$, and $p_i = \chi\nu \exp(-E_M/kT)$, where $\nu$ and $E_M$ are the jump frequency and migration energy, respectively, of a free vacancy and $\chi$ is the coordination number ($\chi = 8$) in the bcc lattice. The vacancy concentration $c_v$ depends on the temperature range.

As long as vacancy loops exist, $c_v$ is obtained from the rate equations

$$\frac{dc_v}{dt} = -p_i c_v c_i - p_l c_v c_l - p_v c_v \tag{2a}$$

(annealing),

$$\frac{dc_v}{dt} = \alpha\phi - p_i c_v c_i - p_l c_v c_l - p_v c_v \tag{2b}$$

(high-temperature implantation), where $\alpha$ is the number of vacancies per incoming impurity available for the migration process described (i.e., $\alpha$ is equal to the number of Frenkel pairs created by each ion, minus those which have recombined with interstitials or formed the initial clusters for vacancy loops), $c_l$ is the concentration of vacancy loops, and $p_v$ and $p_l$ are the probabilities that a vacancy reaches a sink or a vacancy loop, respectively. The latter may be expressed as follows:

$$p_v(p_l) = \zeta(\zeta')\nu e^{-E_M/kT} ,$$

where $\zeta$ and $\zeta'$ are geometrical coefficients[29] to be determined.

At temperatures such that vacancy-loops no longer exist, Eqs. (2) become

$$\frac{dc_v}{dt} = p_d c_l - p_i c_v c_i - p_v c_v , \tag{3a}$$

(annealing),

$$\frac{dc_v}{dt} = \alpha\phi - p_i c_v c_i - p_v c_v \tag{3b}$$

(high-temperature implantation), where $p_d$ is the probability that a vacancy be *released* by a vacancy-loop. This probability will be calculated in Sec. V B. The solution of the coupled differential equations (1) and (2) or (1)–(3) leads to the fraction $z = c_i/c_{i_0}$ (where $c_{i_0}$ is the total impurity concentration) of impurities which remain in initial sites after implantation or annealing at any temperature.

The relation between $z$ and $f$ or $\epsilon$ does not depend on whether annealing or high-temperature implantation is considered, but does depend on the nature of available implanted impurity sites. According to assumption (a), there are three of these. According to II, we have $f = 1$ for impurities in site $i$; when the Yb impurities interact with a defect such as a vacancy (or a vacancy loop) or when they "precipitate" (into clusters, intermetallic compounds, etc.), the HFI is no longer aligned by the exchange field so that for an integral perturbed-angular-correlation (IPAC) measurement $f = 0$. This is the case for sites $l$ and $p$, so that we always have $f = z$. Now consider the channeling results. For each probing beam direction, the extinction ratio $\epsilon$ is the sum, weighted over the site populations, of the extinction ratios appropriate to each site. When vacancy loops exist, no impurity precipitation occurs: $\epsilon = z\epsilon_i + (1-z)\epsilon_l$. At higher temperatures, vacancy-assisted Yb migration leads to "precipitation", $\epsilon = z\epsilon_i + (1-z)\epsilon_p$.

The values of $\epsilon_i$, $\epsilon_l$, and $\epsilon_p$ actually depend on the probing beam direction. Experimentally, $\epsilon_i = 0.56$ in all directions. The value of $\epsilon_p$ must be zero in all directions if the precipitate is incoherent with the iron lattice. If some coherence does exist, $\epsilon_p$ may be different from zero and $\epsilon_p(100)$ may be different from $\epsilon_p$(other directions). We shall study this point in Sec. V B. The parameter $\epsilon_l$ warrants further discussion. When the impurity interacts with a vacancy loop, we shall assume that $\epsilon_l = 0$ except for a (100)-aligned beam. In that case, since the vacancy loops lie in three equivalent (100) planes, two geometries may be defined for impurities in site $l$. One third of the atoms are located in the incoming particle plane (geometry $A$) while the remainder are located in the two equivalent perpendicular planes (geometry $B$). In geometry $A$, a (100)-channeled analyzed particle may meet the rare-earth atom *before* crossing the loop (in which case the impurity should appear substitutional with $\epsilon_l = 1.0$) or *after* crossing the loop (in which case it has picked up enough transverse momentum to be backscattered by the impurity which should appear nonsubstitutional with $\epsilon_l = 0$). We shall assume that the mean value $\epsilon_l(100) = 0.5$ is appropriate for geometry $A$. The impurity is sensed as random in geometry $B$. The expected value of $\epsilon_l$ for a (100)-aligned beam is then $(\frac{1}{3}) \times 0.5 = 0.17$.

### B. Annealing of room-temperature-implanted *Fe*Yb

The experimental results (Fig. 3) were reported previously (see Papers II and III and Ref. 30). Our interpretation is based on the information summarized in Sec. IV, and involves a competition between vacancy trapping by RE impurities or by vacancy loops. As the annealing temperature is raised above the vacancy mobility threshold, the loops grow in their plane [the effect of the (100) plane was first discussed in Ref. 30. It has recently been mentioned in a study of *Fe*I[4]]. This entails a reduction of $1 - \chi_{Fe}$ in the (100) plane [Fig. 3(b)], but no change is observed in the values of $f$ and $\epsilon$. We conclude that when thermally activated, residual *vacancies from the implantation cascades are preferentially trapped by vacancy loops (rather than by RE impurities).* When the temperature is high enough (~720 K), the loops begin to anneal out by releasing vacancies. The fraction $f$ and the ratio $\epsilon$ decrease simultaneously, but the de-

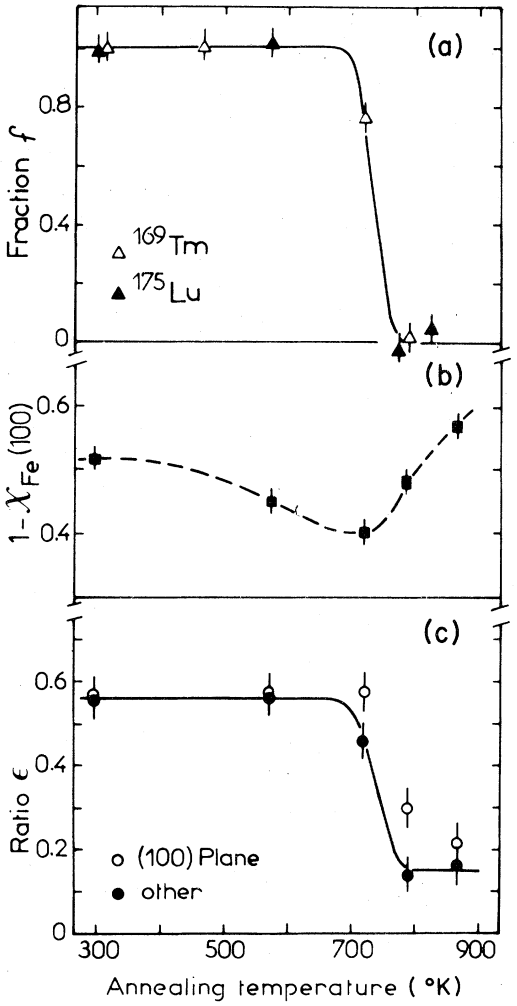


FIG. 3. Annealing properties of Yb-implanted Fe. (a) Fraction $f$ of $^{169}$Tm (open triangles) and $^{175}$Lu (full triangles) nuclei experiencing a magnetic hyperfine interaction (see II). (b) (100)-plane extinction ratio on Fe at Yb-implantation depth. (c) Corrected Yb-extinction ratio $\epsilon$ for the (100) direction (open circles) and for all the other directions studied (full circles). Solid lines are calculated from Eqs. (4) and (6). Broken lines are only to guide the eye.

crease of $\epsilon$ is slower in the vacancy-loop plane. This result suggests that as they anneal out, vacancy loops trap Yb impurities at their periphery (in their strain relaxation area). Complete annealing produces impurity precipitation. As mentioned above, the exact nature of the "precipitate" is unclear but its existence is evidenced by the fact that the Tm spins are no longer aligned by the iron exchange field (see II). The time-differential perturbed-angular-correlation (TDPAC) experiment described in II provides microscopic information on the Yb environment. As "precipitation" takes place and the loops anneal out, the increase of $(1-\chi_{Fe})$ in the (100) plane shows a recovery of the iron lattice (Fig. 3, curve B). We note that the same effects on $f$ and $\epsilon$ would be found if one had vacancy (or divacancy) trapping on the Yb impurity, assuming that for a vacancy (or a divacancy)-impurity pair $\epsilon$ were equal to zero and that the rare-earth spin were "pinned" by a strong crystalline electric field (see Paper II). But as discussed in II, this would not account for the combined results of PAC and Mössbauer experiments on rare earths in Fe. Nor would it account for the privileged influence of the (100) plane.

The fraction $z$ of impurities remaining in sites $i$ after annealing may be deduced straightforwardly from the analysis of Sec. V A. We first consider the temperature range *below* vacancy-loop annealing: the absence of any change in $f$ and $\epsilon$ at the vacancy mobility threshold (preferential trapping of vacancies by vacancy loops rather than by Yb impurities) leads us to neglect the term $p_i c_i c_v$ in Eq. (2a). Electron-microscopy work[23] shows that the number of implantation-induced vacancy loops remains essentially constant ($c_l = c_0$) during annealing in this temperature range, even above the vacancy mobility threshold.[31] Thus, the ratio $z$ is obtained from Eqs. (1a) and (2a),

$$z = \exp\left[\frac{\alpha\phi t_0 p_i}{p_v + p_l c_0}\left(e^{-(p_v+p_l c_0)t} - 1\right)\right] , \tag{4}$$

where $t_0$ is the duration of the implantation ($\sim 10^3$ seconds in all experiments). Since $z$ is not affected [Figs. 3(a) and 3(c)] by vacancy mobility at $T \lesssim 500$ K, where $\exp[-(p_v + p_l c_0)t] \sim 0$, the term in brackets in Eq. (4) must be small; i.e.,

$$\alpha\phi t_0 \chi << \zeta + \zeta' c_0 . \tag{5}$$

The right-hand side of this inequality will be determined from the high-implantation-temperature experiments (Sec. V D), thus setting an upper limit on the room-temperature value of $\alpha$.

In the temperature range *above* the vacancy-loop annealing temperature ($\sim 700$ K) we shall assume for simplicity that the $p_i c_i c_v$ term is negligible in Eq. (3a); i.e., *preferential trapping of vacancies by the surface or other sinks rather than by Yb impurities.* This assumption is quite easy to justify in the case of low-dose implantations for HFI experiments (where $c_i \sim 10^{-5}$); it is debatable for the lattice-location experiment implantations, where $c_i \sim 10^{-3}$. For simplicity, we also assume (as above) that $c_l = c_0$, i.e., that the number and size of the vacancy loops does not change until essentially all the Yb impurities have precipitated. With these approximations,

$$z = \exp[(p_d c_0 p_i / p_v^2)(1 - p_v t - e^{-p_v t})] . \tag{6}$$

This equation describes the change in $z$ above $\sim 700$ K. In view of this result, the fraction $f$ and the ratio

$\epsilon$ will drop simultaneously at $\sim$750 K *only if* $c_0$ *is dose independent* (i.e., identical in our lattice location and HFI implantations). This is in reasonable agreement with the saturation behavior observed in Fe for vacancy-loop densities at implantation doses above $\sim 5 \times 10^{12}$ atoms cm$^{-2}$.[27] The measured loop density at such doses corresponds to $c_0 \sim 10^{-5}$, and we will use this value in the following estimates.

The energy needed to extract a vacancy from a vacancy loop is the sum of a binding energy $E_B$ and of the vacancy migration energy $E_M$; the probability $p_d$ for vacancy release from a loop is proportional to the number of sites $N_c$ on the loop circumference, and

$$p_d = \chi N_c \nu \exp[-(E_M + E_B)/kT] \ .$$

Vacancy-loop size measurements[23] lead to a typical value of $N_c \sim 100$ and an approximate number $n \sim 10^3$ vacancies per loop. A value $E_m = 1.3 \pm 0.1$ eV is obtained from Ref. 26. The value of $E_B$ may be estimated assuming a spherical cluster: the binding energy of a group of $j$ vacancies is then [32]

$$E_B^j(n) = \left[\frac{9\pi}{4}\right]^{1/3} a\gamma_s n^{2/3}\left[\left(\frac{j}{n}\right)^{2/3} - \frac{2}{3}\left(\frac{j}{n}\right)\right] \ ,$$

where $n$ is the number of vacancies in the cluster, $\gamma_s$ is its surface energy, and $a$ is the lattice parameter. With $n \sim 10^3$ and $j = 1$, we obtain $E_B = 1.20$ eV.

Using Eq. (6), the fit (Fig. 3) to the experimental temperature dependence of $f$ and $\epsilon$ is obtained with $\zeta = 10^{-2}$ and $\epsilon_p = 0.18$. As expected, $p_i c_i c_v$ is then indeed negligible for the HFI implantation, but not much smaller than $p_v c_v$ in Eq. (3a) for lattice-location experiments. Although no analytical solution was found in this case, close inspection suggests that the inclusion of this nonlinear term will simply accelerate the drop in $z$ without affecting the temperature range in which it occurs (nor the limiting values of $f$ and $\epsilon$). The value obtained for $\epsilon_p$ indicates some coherence between the Fe lattice and the precipitates formed at high annealing temperatures. As noted above, the higher values of $\epsilon_p$ in the (100) planar direction [Fig. 3(c)] show that Yb impurities are displaced preferentially in this plane.

Our experimental temperature dependence is rather different from that obtained on 80-keV Yb-implanted Fe by Alexander *et al.*[7] although no energy dependence of $\epsilon$ is found on the unannealed samples. As discussed in I, we conjecture that the implanted impurities interact with the surface-oxide layer at the lower implantation energy used in Ref. 7. On the other hand, a temperature dependence identical to ours was obtained in lattice location[3] and HFI[27] experiments on room-temperature implanted 130-keV Xe ions in Fe after annealing up to 800 K. This result suggests that the same mechanisms are operative, and that the effect characterizes the host rather than the impurity. A *dose* dependence of $z$ at room temperature was deduced from a formal rate-equation calculation[33] by Odeurs *et al.*, and found to be in agreement with their experimental results (since we have no information on our site $i$, we are not in a position to discuss the various room-temperature impurity-defect associations ascribed to Xe in Fe from Mössbauer[27] or nuclear-orientation–NMR[34] data).

### C. Implantation of a soluble impurity: Au in Fe

Quite generally, when the annealing temperature is high enough to allow vacancy-assisted impurity migration in iron, we expect to see nonsoluble impurities precipitate or form metallic compounds with zero-hyperfine field (as measured by IPAC) and values of $\epsilon$ near zero. On the other hand, soluble impurities should remain in solid solution upon annealing if they have been implanted in a substitutional site. And when a soluble impurity has been implanted so that it interacts with its damage cascade residue (e.g., a vacancy cluster), vacancy-assisted migration may be expected to facilitate solution and *enhance* $f$ or $\epsilon$.

The lattice-location experiments on Au in Fe described in Paper III were performed in order to check the consistency of this approach (Au is soluble up to 2.7 at.% in Fe). After room-temperature implantation, we find $\epsilon = 0.85$ in agreement with a previously reported[35] value. Upon annealing at 770 K, vacancies released by the Au-implantation-induced vacancy loops foster impurity mobility as described by Eqs. (2a) and (3a). This process, which led to precipitation of insoluble Yb, *improves* the solid solution of Au in Fe and hence increases $\epsilon$ to unity.

### D. High-temperature implantation of Yb in Fe

The experimental results are presented in Fig. 4. The extinction ratio $\epsilon$ drops at the onset of vacancy mobility; the average HFI measured by IPAC still has its room-temperature value when the implantation temperature reaches 570 K, while at the same temperature $\epsilon$ has fallen by a factor of 2 in the (100) direction and a factor of three in other directions. This result cannot be accounted for in terms of Yb precipitation or simple vacancy trapping. The strong planar effect in lattice-location experiments suggests that a large fraction of impurities interact with vacancy loops between 550 and 650 K; we conjecture that vacancy loops are no longer formed above 650 K and that the further drop in $f$ and $\epsilon(100)$ is due to Yb precipitation. Our interpretation is again based on assumptions (a)–(c). The same basic processes [vacancy motion and vacancy-assisted migration as described by Eqs. (1)–(3)] lead to impurity–vacancy-loop interaction below 650 K and

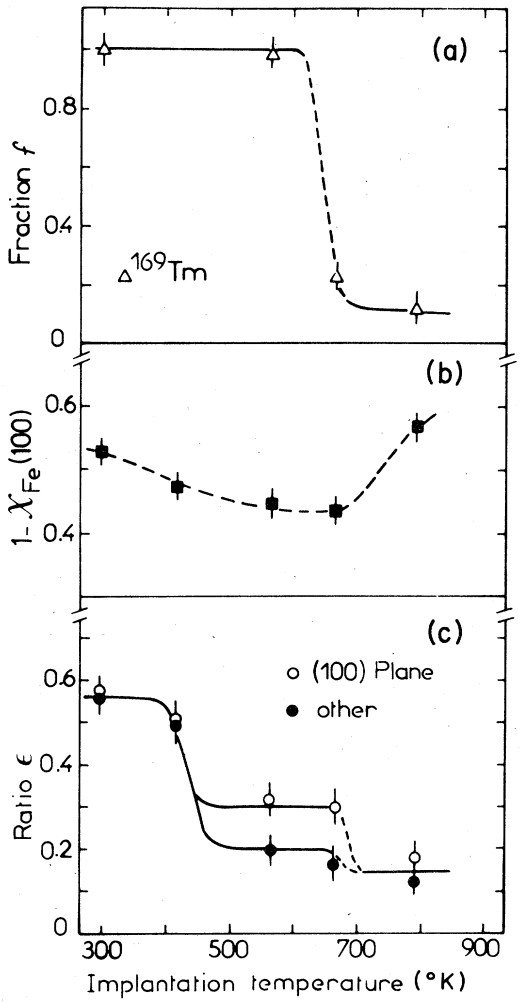


FIG. 4. Change in properties of Yb-implanted Fe with implantation temperature. (a) Fraction $f$ of $^{169}$Tm experiencing a magnetic hyperfine interaction (see II). (b) (100)-plane extinction ratio on Fe at Yb-implantation depth. (c) Corrected Yb-extinction ratio $\epsilon$ for the (100) direction (open circles) and for all the other directions studied (full circles). Solid lines are calculated from Eqs. (7) and (9). Broken lines are only to guide the eye.

to Yb precipitation above that temperature. The two temperature ranges are discussed separately.

*Below 650* K, the time evolution of the impurity population in site $i$ is described by Eqs. (1b) and (2.b). The term $p_i c_i c_v$ is again neglected in Eq. (2b), assuming preferential vacancy capture by vacancy clusters. The resulting coupled equations only offer a simple solution if the approximation $c_i = c_0$ holds, a condition that is now satisfied in *high*-dose (lattice-location) experiments where the vacancy-loop density practically saturates in the very early stages of the implantation, but not in the low-dose (HFI) experiments where $c_i$ increases continuously over most of the implantation time. For the high-dose implantations,

$$z = \left(\frac{1}{ct}\right)\exp\left[-b\left(t+\frac{1}{ce^{-ct}}\right)\right]\sum_{n=0}^{\infty}\left[b^n/c^n n!\left(n-\frac{b}{c}\right)\right] \times [1-\exp(bt-nct)] \quad (T<650\text{K}) \ , \quad (7)$$

where $c = p_v + p_i c_0$ and $b = \alpha\phi p_i/(p_v + p_i c_0)$. Specifically, below the vacancy mobility threshold ($T \lesssim 400$ K) $\exp(-ct) \sim 1$, so that Eq. (7) reduces to $z = 1$. Thus $f = 1$ and $\epsilon = 0.56$. Above the vacancy mobility threshold $\exp(-ct) \sim 0$, so that Eq. (7) goes over to

$$z \simeq (1/bt)[1-\exp(-bt)] \quad (500 < T < 650\text{ K}) \ . \quad (8)$$

Using this Eq. (8), the parameter $b = 2.5 \times 10^{-3}$ is obtained from the experimental values of $\epsilon$ at 570 K. With this value and fitting our results [Fig. 4(c)] in the temperature range up to 650 K with Eq. (7), we obtain $\zeta + \zeta' c_0 = 5 \times 10^{-2}$. In Sec. V B, $\zeta = 10^{-2}$ was derived from the analysis of annealing experiments. With $c_0 = 10^{-5}$, we have $\zeta' = 4000$ and hence all the parameters of the transition probabilities in Eqs. (1)–(3) are known. We may now determine the number ($\alpha$) of vacancies available for Yb-impurity migration. Below the vacancy mobility threshold, this parameter is obtained from Eq. (5) (Sec. V B). For lattice-location experiments, we have $\phi t_0 \sim 10^{-3}$ in concentration terms, so that $\alpha < 1$. This limit agrees with the known[20] maximum damage concentration ($\lesssim 1\%$) in metals. When the implantation temperature is above the vacancy mobility threshold (but below 650 K), the total concentration of vacancies is large, but most are trapped by vacancy loops. From Eq. (8), the value of $\alpha$ is then $\alpha \sim 20$.

Equation (8) provides a lower limit of the value of $z$ for the low-dose implantations below 650 K, hence an estimate of the maximum expected change in $f$ in that temperature range. With the appropriate values of $\zeta$, $\chi$, $\phi t = 10^{-5}$ and $\alpha = 20$, we find $z > 0.92$. Therefore $f > 0.92$ and $\epsilon > 0.51$ as long as the implantation temperature is below 650 K. This is in agreement with our results.

We may also compare Eq. (8) to the results of high-temperature-implantation experiments[27] on Xe in Fe. These were Mössbauer HFI experiments, for which the implanted doses were comparable to those of our lattice-location experiments (typically $10^{14}$ atoms cm$^{-2}$). In that case, the amplitude of the HFI component identified as the "substitutional fraction" (corresponding to our "initial site" denomination) drops to zero at 470 K. This is in excellent agreement with the prediction of Eq. (8).

*Above 700* K, if vacancy clustering no longer takes

place, the evolution of the system is described by Eqs. (1b) and (3b). Assuming as previously that vacancies are preferentially trapped by sinks other than the Yb impurities (and since $c_0=0$), the solutions of these equations are identical to Eq. (7), but the values of $b$ and $c$ are now $b=\alpha\phi p_i/p_v$ and $c=p_v$. Since we are far above the vacancy mobility threshold, the solution reduces to

$$z=(\alpha\phi p_i t/p_v)^{-1}[1-\exp(-\alpha\phi p_i t/p_v)] \quad (T>700\ \text{K})\ . \tag{9}$$

Assuming that the high-temperature value of $f$ in Fig. 4 is due to Yb impurities remaining in initial sites, we may determine the value of $\alpha$ in the temperature range where vacancy clustering no longer occurs (using the previously deduced values of $\zeta$ and $\chi$). We find $\alpha\sim 700$, in reasonable agreement with the value expected from a calculation of the average number of Frenkel pairs produced per ion using the modified[36,37] Kinchin-Pease formula.

For the high-dose experiments above 700 K, the value of $z$ calculated from Eq. (8) using $\alpha=700$ is zero: in our experiments, all the Yb impurities have precipitated. In order to obtain agreement with the experimental value of $\epsilon$ in all directions [Fig. 4(c)], the value of $\epsilon_p$ must be $\sim 0.18$, as in the annealing experiment discussed in Sec. V B. This indicates that Yb precipitates have the same structure in both experiments.

Our interpretation of the process occurring in the temperature range 560–700 K does not lend itself to calculation within the simple model described in the preceding paragraphs. We assume that migrating vacancies no longer form vacancy clusters when $kT$ is about equal to the sum of the vacancy migration energy $F_M$ and of the binding energy $E_B'$ of the smallest stable vacancy cluster. From the experimental data, we deduce $E_B'\sim 0.5$ eV, a reasonable value[38] for a group of four vacancies (often considered to be the smallest stable cluster). Since $E_B'$ is smaller than the binding energy of a vacancy in a large cluster, Yb precipitation occurs at lower temperatures in high-temperature implantation than in annealing experiments.

It is interesting to compare our analysis to that[33] of Odeurs *et al.*, who attempted a general formulation of impurity-site evolution in implantation experiments. The latter work assumed transition probabilities between unspecified implanted impurity sites under equilibrium conditions. Thus, reversible processes (transitions site $i\rightleftarrows$site $j$) were included. The results were applied to the dose dependence of the HFI change at Xe in Fe. As discussed above, the nature of the impurity-defect interaction in our experiments leads us to consider only irreversible transitions and our calculation accounts for the annealing and high-temperature-implantation dependence of both the HFI and lattice-location properties. Considering the properties of defects in Fe specifies (and considerably simplifies) our analysis, but it is easy to see that the rate equations of Ref. 33 may reduce to Eq. (7) if appropriate transition probabilities are assumed. Both approaches are actually hampered by the assumption (basic to any equilibrium-thermodynamical calculation) of a uniform initial defect distribution. To our knowledge, no calculation (such as Ref. 39) involving the correlation between the stopping ion and its associated defects has been applied to experimental analysis.

## VI. CONCLUSION

Several features of the present discussion are perhaps worth underlining. Firstly, the interesting correlation (in the absence of damage evolution) between $\epsilon$ and the implanted-impurity atomic radius warrants an explanation. It would be of significance to know whether it is due solely to the impurity-induced lattice strain or to the elastic impurity-defect attraction: this could help to interpret many lattice-location results. Secondly, the annealing and high-implantation-temperature experiments demonstrate the importance of radiation damage evolution in lattice-location and HFI measurements. We have shown that the various temperature dependences observed in all our experiments may be accounted for simultaneously with a simple model of radiation-damage evolution. The results are found to account for results of other experiments (where available) as well. It should be noted that under our assumptions, impurity evolution occurs via a two-step mechanism: vacancy migration towards the impurity followed by vacancy-assisted impurity migration. We assumed everywhere that the latter process is fast compared to the former, so that all our equations involve vacancy migration to the impurity. Thus the model presented here may very well be valid even if some other second stage were preferred to vacancy-assisted migration (as long as this second stage is much faster than the first). We submit that our results establish the importance of the vacancy-impurity interaction. The structure of the impurity-vacancy complex (i.e., whether it involves one or several vacancies) remains to be determined. So do the details of its migration process, for which only the influence of the (100) plane was established here.

## ACKNOWLEDGMENTS

We are indebted to J. Chaumont, N. V. Doan, L. Kubin, Y. Lévy, Y. Quéré, and M. O. Ruault for discussions and comments, and to R. B. Alexander and J. Odeurs for communication of their results prior to publication. This work was partially supported by CNRS under Recherche Cooperative Sur Programme (R.C.P.) Grant Nos. 157 and 185.

*This work is part of a Ph.D. thesis submitted by L. Thomé to Université Paris-Sud, Orsay.

[1]L. Thomé, H. Bernas, F. Abel, M. Bruneaux, C. Cohen, and J. Chaumont, Phys. Rev. B 14, 2787 (1976); hereafter called I; L. Thomé, H. Bernas, and R. Meunier, Phys. Rev. B 20, 1771 (1979) (second preceding paper), hereafter called II; C. Cohen, L. Thomé, F. Abel, M. Bruneaux, J. Chaumont, and H. Bernas, Phys. Rev. B 20, 1780 (1979) (preceding paper), hereafter called III.

[2]H. de Waard and L. C. Feldman, in *Applications of Ion Beams to Metals,* edited by S. T. Picraux, E. Eer Nisse, and F. Vook (Plenum, New York, 1974), p. 317.

[3]L. C. Feldman and D. Murnick, Phys. Rev. B 5, 1 (1972).

[4]P. T. Callaghan, P. K. James, and N. J. Stone, Phys. Rev. B 12, 3553 (1975).

[5]P. T. Callaghan, P. Kittel, N. J. Stone, and P. D. Johnston, Phys. Rev. B 14, 3722 (1976).

[6]J. R. Mac Donald, R. A. Boie, W. Darcey, and R. Hensler, Phys. Rev. B 12, 1633 (1975).

[7]R. B. Alexander, E. J. Ansaldo, B. I. Deutch, J. Gellert, and L. C. Feldman, Hyp. Int. 3, 45 (1977).

[8]R. L. Cohen, B. Beyer, and B. I. Deutch, Phys. Rev. Lett. 33, 518 (1974).

[9]L. Thomé, H. Bernas, J. Chaumont, F. Abel, M. Bruneaux, and C. Cohen, Phys. Rev. Lett. A 54, 37 (1975).

[10]L. Niesen, Hyp. Int. 2, 15 (1976), and references therein.

[11]H. P. Wit, Ph.D. thesis (University of Groningen, 1976) (unpublished).

[12]*Channeling: Theory, Observation and Applications,* edited by D. V. Morgan (Wiley, New York, 1973).

[13]Y. Quéré, Radiat. Eff. 28, 253 (1976).

[14]R. B. Alexander, P. T. Callaghan, and J. M. Poate, Phys. Rev. B 9, 3022 (1974).

[15]W. Hume-Rothery, R. E. Smallman, and C. W. Haworth, *The Structure of Metals and Alloys* (Institute of Metals, London, 1969).

[16]E. N. Kaufmann, J. M. Poate, and W. M. Augustyniak, Phys. Rev. B 7, 951 (1973).

[17]D. K. Sood and G. Dearnaley, J. Vac. Sci. Technol. 12, 463 (1975).

[18]J. A. Borders and J. M. Poate, Phys. Rev. B 13, 969 (1976).

[19]A. Seeger, in *Second International Conference on Peaceful Uses of Atomic Energy, Geneva* (IAEA, Vienna, 1958), Vol. b, p. 250.

[20]W. Schilling, G. Burger, K. Isebeck and H. Wenzl, in *Vacancies and Interstitials in Metals,* edited by A. Seeger, D. Schumacher, W. Schilling, and J. Diehl (North-Holland, Amsterdam, 1970), p. 255.

[21]W. Glaeser and H. Wever, Phys. Status Solidi 35, 367 (1969).

[22]N. Yoshida, M. Kiritani, and F. E. Fujita, J. Phys. Soc. Jpn. 39, 170 (1975).

[23]H. Bernas, M. O. Ruault, and B. Jouffrey, Phys. Rev. 27, 589 (1971); and M. O. Ruault, H. Bernas, and J. Chaumont, Philos. Mag. (to be published).

[24]Existence of stable ⟨100⟩ loops in Fe after heavy ion irradiation has also been demonstrated by M. L. Jenkins, C. A. English, and B. L. Eyre, Philos. Mag. A 38, 97 (1978).

[25]M. Lerme, Thèse 3*e* cycle (University of Toulouse, 1978) (unpublished).

[26]See for example: *Physics of Irradiation-Produced Voids,* edited by R. S. Nelson, AERE Report R7934 (1975) (unpublished).

[27]S. R. Reintsema, S. A. Drentje, P. Schurer, and H. De Waard, Radiat. Eff. 24, 145 (1975); S. R. Reintsema, Ph.D. thesis (University of Groningen, 1976) (unpublished).

[28]J. Burke, J. Less-Comm. Met. 28, 441 (1972).

[29]A. C. Damask and G. J. Dienes, *Point Defects in Metals* (Gordon and Breach, New York, 1963).

[30]F. Abel, M. Bruneaux, C. Cohen, H. Bernas, J. Chaumont, and L. Thomé, Solid State Commun. 13, 113 (1973); see Ref. 2, p. 377.

[31]In I, we found that the dose dependence of lattice-location and HFI results obtained on oxygen-implanted *Fe*Yb systems could only be accounted for if oxygen atoms were trapped in sinks whose efficiency was proportional to the Yb dose. It was suggested that the oxygen sinks were vacancy loops, and hence we were led to assume that their concentration was Yb dose-proportional even at high ($5 \times 10^{14}$ atoms cm$^{-2}$) doses. The fact that this is in contradiction to experimentally observed[23] saturation in the $10^{12}$–$10^{13}$ atoms cm$^{-2}$ range was unfortunately overlooked. Actually, the oxygen sinks need not be vacancy loops (the complex dislocation network of heavily implanted samples suggests that oxygen may be trapped very efficiently). Such sinks may play a major role in oxygen trapping, while being of negligible efficiency, compared to vacancy loops, for vacancy trapping. The analysis of the Yb-O presented in I then remains valid.

[32]A. Sigher and D. Kuhlmann-Wilsdorf, Phys. Status Solidi 21, 545 (1967).

[33]J. Odeurs, R. Coussement, and H. Pattyn, Hyp. Int. 3, 461 (1977).

[34]E. Schoeters, R. Coussement, R. Geerts, J. Odeurs, H. Pattyn, R. E. Silverans, and L. Vanneste, Phys. Rev. Lett. 37, 302 (1976).

[35]R. B. Alexander, N. J. Stone, D. V. Morgan, and J. M. Poate, in *Hyperfine Interactions in Excited Nuclei,* edited by G. Goldring and R. Kalish (Gordon and Breach, New York, 1971), p. 229.

[36]P. Sigmund, Appl. Phys. Lett. 14, 114 (1969).

[37]I. M. Torrens and M. T. Robinson, in *Interatomic Potentials and Simulation of Lattice Defects,* edited by P. C. Gehlen, J. R. Beeler, and R. J. Jaffee (Plenum, New York, 1972), p. 423. Note that the appropriate displacement energy $E_d$ to use here in the familiar Kinchin-Pease equation is not the threshold energy, but the energy for which the displacement probability approaches unity. The latter is easily twice as large as the former.

[38]J. R. Beeler and R. A. Johnson, Phys. Rev. 156, 677 (1967).

[39]J. E. Westmoreland and P. Sigmund, Radiat. Eff. 6, 187 (1970).